IOPscience iopscience.iop.org

Home Search Collections Journals About Contact us My IOPscience

An investigation of the temporal evolution of plasma potential in a 60 MHz/2 MHz pulsed dual-frequency capacitively coupled discharge

This article has been downloaded from IOPscience. Please scroll down to see the full text article.

2012 Plasma Sources Sci. Technol. 21 055006

(http://iopscience.iop.org/0963-0252/21/5/055006)

View the table of contents for this issue, or go to the journal homepage for more

Download details:
IP Address: 115.145.196.92
The article was downloaded on 20/08/2012 at 01:58

Please note that terms and conditions apply.

Plasma Sources Sci. Technol. **21** (2012) 055006 (9pp) doi:10.1088/0963-0252/21/5/055006

An investigation of the temporal evolution of plasma potential in a 60 MHz/2 MHz pulsed dual-frequency capacitively coupled discharge

Anurag Mishra[1], **Min Hwan Jeon, Kyong Nam Kim**[1] **and Geun Young Yeom**[1,2]

[1] Department of Advanced Materials Science and Engineering, Sungkyunkwan University, Suwon, Gyeonggi-do, 440-746, South Korea
[2] SKKU Advanced Institute of Nanotechnology(SAINT), Sungkyunkwan University, Suwon, Gyeunggi-do 440-746, South Korea

E-mail: gyyeom@skku.edu

Received 6 March 2012, in final form 12 July 2012
Published 17 August 2012
Online at stacks.iop.org/PSST/21/055006

Abstract
Using an electron-emitting probe, time-resolved plasma potential (V_p) measurements are carried out in a pulsed dual-frequency 60 MHz/2 MHz capacitively coupled discharge. The discharge is produced using argon gas at two chosen pressures of 20 and 40 mTorr, a duty ratio of 50% and pulse powers ranging from 100 to 500 W. The pulsing frequency is set at 1 kHz. The plasma potential measurements are carried out at 10 mm above the centre of the substrate.

It is observed that V_p follows the source discharge pulse voltage and remains positive during the whole pulse cycle. Without substrate biasing, the prominent features observed in the V_p profile, under all the operating conditions, remain similar; however, the magnitude of V_p increases with the applied RF source power. For further analysis, three distinguishable features in the V_p profile, a transient spike at the beginning of the discharge pulse, a stable 'on-phase' and a 'stable-off' phase, are identified. For typical operating conditions (20 mTorr and 500 W), the transient spike in V_p of ~30 V appears for 30 μs, then it attains a stable value of ~12 V during the rest of the pulse on-period. V_p decreases up to ~3 V as the pulse is switched off.

It is also observed in this study that a continuous wave RF biasing of the substrate significantly modulates the plasma potential evolution, specifically when the pulse is switched off and the magnitude of modulation depends on the substrate biasing power. The temporal evolution of electron temperature derived from the plasma and floating potentials is also reported.

1. Introduction

Parallel-plate capacitively coupled plasma (CCP) discharges are being extensively used in the microelectronics industry for deposition and dry etching [1–7]. However, this technique lacks separate control over the plasma production mechanism, i.e. plasma density and ion-bombarding energy over the substrate. A solution to this problem is the application of two different frequencies, high and low, on the top and bottom electrodes, respectively. This modified technique is known as a dual-frequency capacitively coupled plasma (DF-CCP) discharge. In this technique, a higher frequency (ranging from a few tens of MHz to a few hundred MHz) is applied on the top electrode and a lower frequency (typically 2 MHz, ranging from a few to 10 MHz) on the bottom electrode. The application of dual frequencies facilitates separate control over the plasma density and ion-bombarding energy over the substrate; plasma density is controlled by the higher frequency, and the ion-bombarding energy by the lower frequency. Further flexibility in the DF-CCP can be

 © 2012 IOP Publishing Ltd Printed in the UK & the USA

introduced by the application of pulsed RF on the top electrode or both electrodes. The application of a very high frequency (such as 60 MHz or more) on the top electrode produces a reduced ion-bombarding energy and thinner sheath for a given ion flux to the substrate, that, in turn, could be useful for low-damage dry etching applications. The higher frequency produces a higher plasma density ($n_e \propto \omega^2 V_{rf}$) and the total potential ($|V_h + V_l|$) determines the ion-bombarding energy. Therefore, for separate control over plasma density and ion-bombarding energy, ($\omega_h^2|V_h| \gg \omega_l^2|V_l|$) should be satisfied. If ($|V_l| \gg |V_h|$), the low frequency gives good control over the ion-bombarding energy over the substrate.

The DF-CCP has been a subject of intense research in recent years. Various theoretical, computational and experimental studies have been carried out to reveal the underlying physics and to optimize the operational conditions. Using a homogeneous plasma model for dual-frequency RF discharges, and under the assumptions of time-independent collisionless ion motion and inertialess electrons, a computational study was carried out, and it was shown that the discharge parameters are a function of effective parameters such as effective frequency, effective current and effective voltage and these effective parameters are determined by the ratio of two currents and voltages [8]. They also reported that when determining the plasma parameters, the reduction in the size of the bulk discharge due to two sheaths has to be taken into account [9]. Another computational study, using the PIC-MCC simulation, revealed that the ion flux and the ion-bombarding energy over the substrate can be separately controlled. They mentioned two different controlling parameters for two different operational regimes of small and large electrode separations. At large electrode separation, the ion current is a function of the total discharge current, whereas at small electrode separation, the ion flux can be controlled by varying the power at the high frequency. However, in both cases the ion-bombarding energy depends on the low-frequency voltage. The ratio of the two frequencies plays a vital role in controlling the ion impact and plasma density in DF-CCPs [10]. If the ratio of high frequency to low frequency is sufficiently high, independent control is possible by manipulating the high- and low-frequency sources. Using the hybrid model composed of fluid and Monte Carlo models, Dai *et al* [11] showed that the bias frequency, power of the low-frequency source and pressure play an important role in determining collisional dual RF sheaths and therefore ion energy and angular distributions over the substrate. By developing an analytical model, Turner *et al* [12] predicted that the net heating in a dual-frequency CCP discharge is larger than the sum of the effects occurring when the two frequencies are applied separately. This prediction has been supported by kinetic simulation. In another study, Turner *et al* [13] showed that electron heating in a DF-CCP discharge also depends parametrically on the lower frequency, contrary to common supposition. Various other theoretical and computational studies [8–20] have been performed to provide better physical insight into the physical processes occurring in DF-CCP discharges. Rauf *et al* [21] computationally investigated that electrostatic effects dominated in electronegative plasmas because the applied RF potential is considerably larger for the same power compared with electropositive plasmas.

In an experimental study carried out using a hairpin probe [22], it was demonstrated that plasma density is a linear function of the high-frequency power. However, it also depends marginally on the low-frequency power, in contrast to the reported particle-in-cell computational study [10]. A mass energy-resolved spectrometric [22] study together with numerical simulations demonstrated that the low frequency and low-frequency power have a significant effect on the high-energy peak in ion energy distribution and it shifts towards the high-energy region with increasing low frequency and power at the low frequency. A diagnostics study was carried out by Hebner *et al* [23] in single-frequency and DF-CCP discharges operating in argon and driven at frequencies between 10 and 190 MHz. They reported that, while keeping the lower electrode grounded, the spatial distribution of argon ions changed from uniform to centre peaked as the excitation frequency was increased on the top electrode. At a pressure of 50 mTorr and a frequency of 60 MHz, they observed that with increasing power (300–1000 W) the electron density changed from being uniform as a function of radius to being centre peaked. These observations may be explained on the basis of constructive interference of the plasma shortened wavelength with increasing electron density and conductivity. Using a Langmuir probe and V–I probe measurements [24], an experimental study was carried out by varying the frequency ratio, system pressure, high frequency and low frequency. Both frequencies were applied at the top electrode, and the bottom electrode was grounded. They reported that an increase in the low-frequency power causes a moderate increase in the electron density but a significant decrease in the electron temperature. And an increase in the high-frequency power results in a strong increase in the electron density and populates the high-energy part of the electron energy distribution functions. Various other experimental studies strengthen these findings [25–27].

Recently, pulsed DF-CCP discharges have attracted significant research interest in academia and industry due to increased flexibility in operational conditions, thus allowing one to tailor the discharge properties for a particular application. The pulsed operation of the discharge significantly prevents the formation of arcs and therefore the discharge is much more stable whereby the quality of etching is enhanced. The periodic interruption of the driving frequency leads, on the other hand, to strong temporal changes in the plasma parameters, which make a physical description of these types of discharges even more difficult. Therefore, there is a need for systematic experimental investigation to understand the discharge dynamics and temporal evolution of plasma parameters. This would not only provide a better physical insight but would also give information about the operation conditions appropriate for a particular application. However, there is a clear lack of studies on the temporal evolution of plasma parameters in pulsed DF-CCP discharges.

One of the important discharge parameters is the plasma potential, V_p, in the discharge volume. It determines the electric field that accelerates the electrons to sustain the

discharge, and is therefore crucial for the discharge formation. On the other hand, the value of the plasma potential in front of each electrode or the wall at a fixed potential determines the ion-bombarding energy with which the ions hit the surface and controls the charge flux to the electrodes. Therefore, knowledge of the temporal evolution of plasma potential is directly important for dry etching as long as the substrate is not at a floating potential, which adjusts itself according to the plasma potential and the electron energy.

The electron temperature, T_e, is also a very important discharge parameter which, together with plasma density, determines the discharge chemistry and therefore plays a vital role in etching and selectivity. The electron temperature, T_e, determines the ionization, dissociation and excitation rates in the plasma, as well as the energy and ion flux to the substrate. Therefore, information about the temporal evolution of T_e is of great importance for understanding the plasma behaviour and optimizing the plasma processes. There are a few studies on T_e measurements conducted in an Ar CCP [32–34]. Descoeudres *et al* [35] reported a value of 6 eV at a pressure of 76 mTorr and 4.8 eV at 200 mTorr in a 13.56 MHz single-frequency discharge with a gap of 4 cm. So *et al* [36, 37] modelled a 200 mTorr, 13.56 MHz CF_4 CCP with a 2 cm gap and computed a T_e of 6 eV in the bulk plasma. Using the trace rare gas optical emission spectroscopy (TRG-OES) technique, Chen *et al* conducted an experimental study in a DF-CCP discharge of CF_4+O_2 and reported electron temperature variation with power, pressure and various percentages of operating gases. They observed an increase in electron temperature with RF power and pressure [6].

This study investigates the temporal evolution of plasma potential and its dependence on bias power and operating pressure in a 60 MHz/2 MHz pulsed DF-CPP discharge and its dependence on bias power, duty factor and pulsing frequency. The diagnostic technique used was an emissive probe in the 'floating point method' (yielding a direct measurement of V_p on the oscilloscope screen), which is valid provided that the probe is maintained in the full emission condition. The principle is based on an ordinary Langmuir probe technique. When the probe tip is appropriately heated via a 50 Hz ac current, it emits electrons, which act as an apparent additional positive ion current drawn by the probe from the plasma. The floating potential measured by such a probe thus approaches the plasma potential and serves as a good measure for it—in an ideal case with an error of the order of kT_p/e, where T_p is the probe temperature, provided that the probe is in the strong emission condition. In the case of space charge effects, this technique underestimates V_p by T_e/e. Therefore, it gives fairly good estimates of V_p, if the plasma temperature is small ($eV_p/T_e \leqslant 1$) [38]. The advantage of the method is that it is not necessary to acquire the complete characteristics to obtain the plasma potential; rather it can be accessed from a single measurement of the floating potential, which is easily obtained through a high-impedance measurement against ground. With this measurement being performed with an oscilloscope, a time-resolved determination of varying plasma potentials is possible. Details of using an emissive probe in a pulsed plasma can be found elsewhere [28, 29].

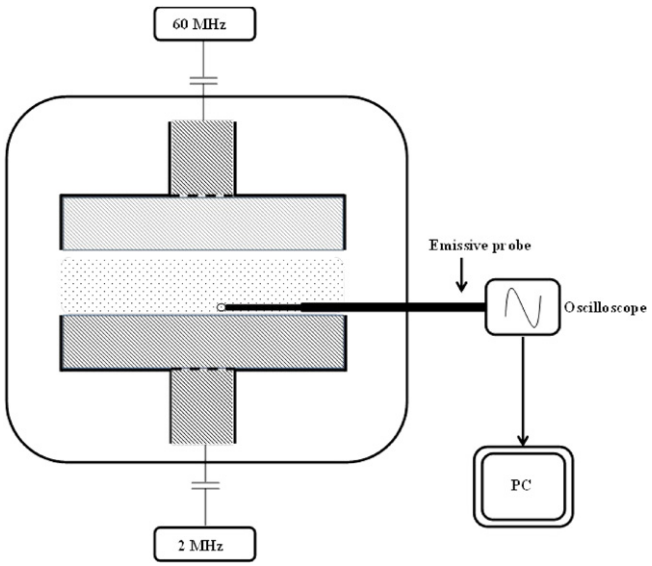

Figure 1. A schematic of the experimental setup of the pulsed dual-frequency capacitively coupled discharge chamber used in this study. The top electrode was energized by pulsed 60 MHz RF power and the bottom electrode was energized with continuous wave 2 MHz RF power.

The emissive probe could also be used to estimate the electron temperature using the difference between the floating potentials of the probe when it is cold and in strongly emitting conditions [41, 42]. Therefore, these emissive probe measurements were also used to estimate the time-resolved electron temperature, which was derived from the relation of electron temperature with the plasma and floating potentials.

2. Experimental arrangement

The schematic of the experimental setup of the DF-CCP system used in this study is shown in figure 1. Experiments were performed in a purpose-built chamber made of anodized aluminum of external dimension $600 \times 600\ mm^2$. The internal diameter of the chamber was 300 mm. The argon gas discharge was maintained between two 200 mm diameter parallel-plate electrodes separated by 30 mm at two average pressures of 20 and 40 mTorr, a duty factor of 50% and a pulsing frequency of 1 kHz. The top electrode was covered with a perforated silicon plate to act as a shower head and thus to allow the gas to spread uniformly. The top electrode was capacitively connected to a 60 MHz RF power source (HF) together with a pulsing unit with the facility of varying the pulsing frequency and duty factor. The bottom electrode was capacitively connected to a 2 MHz RF power source (LF). The reactor was evacuated using an EBARA turbo molecular pump of pumping speed $3200\ l\ s^{-1}$ backed by a booster and rotary pump supplied by Alcatel. The base pressure continuously achieved by this pumping unit was 2.0×10^{-5} Torr. The gas was equally distributed through a baffle system from the top electrode. A tight steel mesh block was installed around the bottom electrode to reduce the plasma leakage by the pumping system connected to the bottom of the chamber. The process pressure was controlled automatically by adjusting a throttle valve.

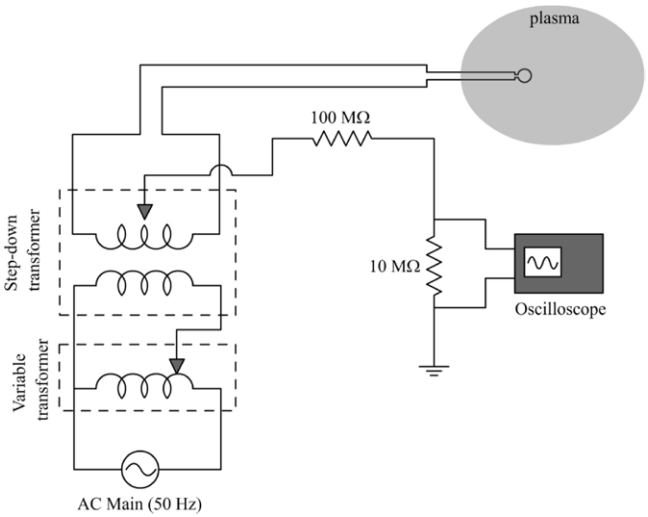

Figure 2. A schematic of the emissive probe electrical arrangement.

The emissive probe electrical arrangement is shown in figure 2. The emissive probe itself was made of a thoriated tungsten wire of diameter 125 μm, looped in a semicircle of 2 mm diameter and push-fitted into a ceramic stem housing with enamelled copper connecting wires of 250 μm diameter that carry the external heating current. The probe loop was heated by passing a 50 Hz ac current through it supplied by a two-stage transformer circuit. The centre tap of the second transformer was connected to a fast oscilloscope (TDS 744, 10 M input impedance, Tektronix Ltd) via a single-strand wire (used to minimize the capacitance to ground) to obtain the mean voltage (floating potential) across the loop and hence a good estimate of V_p. These floating potential data were stored over 128 discharge pulses and then averaged to minimize the random error in the electrical signal. The emissive probe was located at the centre and 10 mm away from the substrate. Before carrying out actual measurements, some preliminary measurements were performed to verify the required probe loop current to be in the state of strong emission, and it was found that the 0.9 A current is enough to get strong emission during the whole pulse cycle.

3. Results and discussion

The temporal evolution of plasma potential (in the strong emission condition) and floating potential (in the zero emission condition) acquired by the emissive probe, measured at a pulse power of 200 W, and an average pressure of 20 mTorr, is shown in figure 3. The emissive probe was located at a particular position of the substrate ($r = 0$ mm and $z = 10$ mm). The plasma potential gets a significant spike of ~60 V at the beginning of the pulse, which temporally coincides with the beginning of the RF pulse at the top electrode. Subsequently, the plasma potential decreases sharply and later on, after ~50 μs, attains a stable value of ~30 V for the rest of the pulse 'on-time'. As the pulse is switched off, the plasma potential decreases rapidly and attains a small positive value of ~5.5 V within 25 μs and remains constant for the rest of the pulse. For an in-depth analysis, three features on the V_p profile

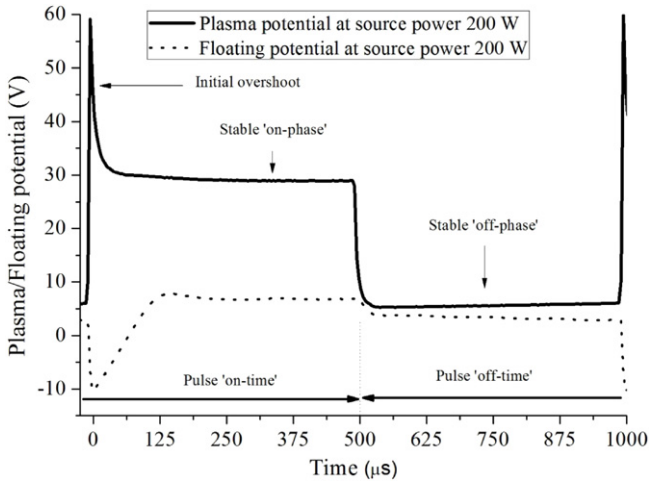

Figure 3. Potential profile measured with the emissive probe for two different conditions: (black) strongly heated at $(r, z) = (0\,\text{mm}, 10\,\text{mm})$, (red) no heating at $(r, z) = (0\,\text{mm}, 10\,\text{mm})$. The discharge was pulsed at 1 kHz with 50% duty factor.

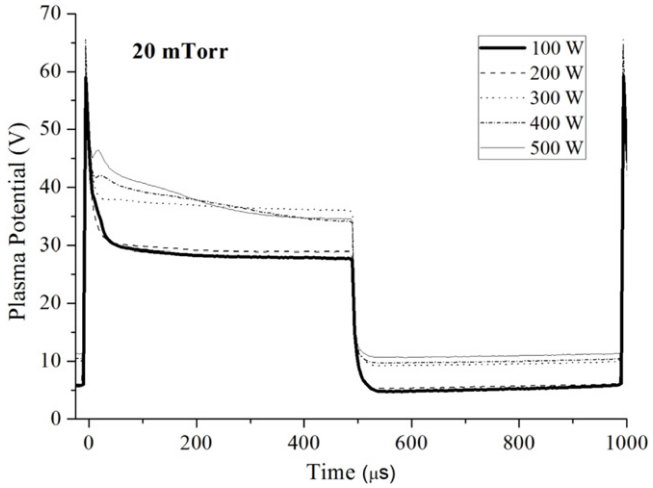

Figure 4. Potential profile measured with the emissive probe for five different source powers at an average pressure of 20 mTorr. The discharge was pulsed at 1 kHz with 50% duty factor. The bias power was zero.

were identified as an 'initial overshoot' (within a few μs of the initiation of the pulse), a stable 'on-phase' (~50 μs after the initiation of the pulse) and a stable 'off-phase' (~25 μs after switching off the pulse), as shown in figure 3.

Figure 4 shows the plasma potential profiles measured at five different source powers ranging from 100 to 500 W at an average pressure of 20 mTorr. The bottom electrode was grounded. The dominant features in all the potential profile are similar; however, their magnitude varies with applied power. As the pulse is switched on, the plasma potential gets an initial overshoot of ~70 V; its exact magnitude depends on the average power fed to the plasma. This initial overshoot relaxes within a time of ~25 μs and then maintains a stable 'on-phase' of a few tens of volts. The plasma potential rapidly goes down as the pulse is switched off and maintains a few volts above the ground level for the entire pulse 'off-phase'. The observed variation in plasma potential with RF power can be explained as follows. When an RF power is applied to the

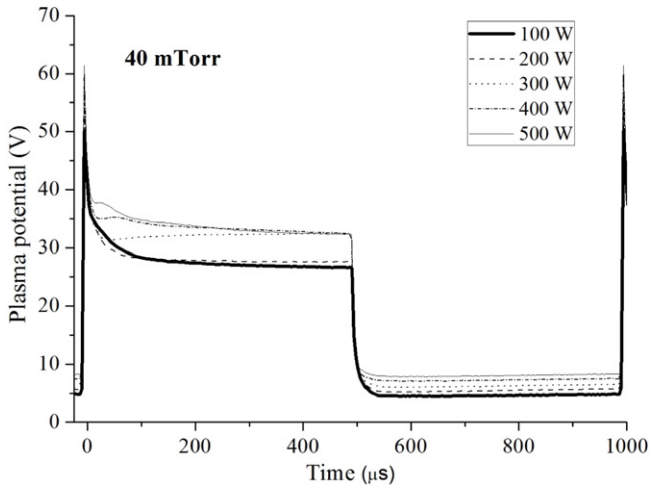

Figure 5. Plasma potential profile measured with the emissive probe for five different source powers at an average pressure of 40 mTorr. The discharge was pulsed at 1 kHz with 50% duty factor. The bias power was zero.

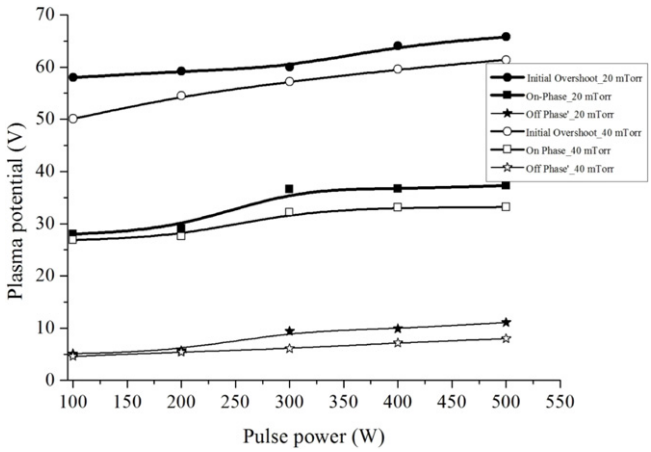

Figure 6. Plots of V_p versus pulse power for the three phases identified in figure 3: (*a*) the 'initial overshoot', (*b*) the 'stable on-phase' and (*c*) the 'stable off-phase'. The continuous lines with solid circles are for 20 mTorr and the continuous lines with solid stars are for 40 mTorr.

electrode, the instantaneous plasma potential is given by [30]

$$\eta_S = \ln\left[\frac{1+\delta\exp(\eta_G \sin\omega t)}{(1+\delta)\varepsilon}\right], \qquad (1)$$

where $\eta = eV/kT_e$, the subscripts S and G are used for space and the grounded electrode, respectively, δ is the ratio of the area of the powered electrode to the grounded electrode and $\varepsilon = [\pi m/2M]^{1/2}$. From this equation, it can be easily concluded that, as the RF power is increased, the sinusoidal oscillation applied to the powered electrode also increases. As the plasma potential follows the most positive surface immersed in the discharge body, it increases with increasing applied power.

The same measurements carried out at an average pressure of 40 mTorr (higher pressure) are shown in figure 5. A comparison of figures 4 and 5 readily reveals that the plasma potential is marginally dependent on the pressure [31]. This observed slight reduction in the plasma potential could be attributed to the change in the plasma density and electron temperature due to the increased pressure.

At the beginning of the discharge pulse, the emergence of a small bump in the V_p profile at time $t \sim 5\,\mu$s was observed (figures 4 and 5). It could be attributed to the discharge dynamics at the beginning of the pulse, probe response to it and the complex reactance of the probe measurement circuitry.

Two peaks are observed in a typical plasma potential profile; the first one occurs at $t < 1\,\mu$s and the second one at $t \sim 5\,\mu$s. Assuming the plasma density to be $\sim 10^{15}$ m^{-3}, the characteristic time scales of electron and ion motion calculated from the inverse electron plasma frequency (f_e) and ion plasma frequency (f_i) are $\tau_e \sim 5$ ns and $\tau_i \sim 1\,\mu$s, respectively. As the discharge pulse is switched on, there is a sudden acceleration of emitted electrons situated in the space charge region around the probe loop to the plasma. It generates a peak in the plasma potential at a time of approximately a few ns. In this very short time (τ_e), the ions are immobile and therefore there is no contribution due to ion motion in the first peak.

As the discharge builds up, the flow of electrons from the probe loop to the plasma slows down and it generates a rapid fall in the plasma potential.

The ions respond at their characteristic time scale (τ_i), namely of a few μs. The second small peak (bump) in the plasma potential profile could be attributed to the ion response to the probe.

For an in-depth analysis of the time evolution of plasma potential, and plasma potential dependence on RF power and pressure, the plasma potentials at three chosen points (initial overshoot, stable 'on-phase' and stable 'off-phase') are plotted and shown in figure 6. From the figure, it is clear that the plasma potential slightly decreases with increasing pressure in all three phases. In the stable 'on-phase' and the stable 'off-phase', there is almost no change in the plasma potential when the applied RF pulse power is below 200 W ($P < 200$ W). However, the plasma potential increases with pulse power beyond 200 W.

The temporal evolution of electron temperature was qualitatively estimated using the following relation between plasma potential and floating potential [30]:

$$V_p - V_f = \frac{kT_e}{2e}\ln\left(\frac{\pi m}{2M}\right), \qquad (2)$$

where V_p and V_f are the plasma and floating potentials, respectively, T_e is the electron temperature, m is the electronic mass and M is the atomic mass of the discharge gas. Thus calculated, for argon gas, the difference in plasma and floating potentials ($V_p - V_f$) amounts to 5.38. The electron temperature profile, thus obtained, is shown in figures 7 and 8 for pressures of 20 mTorr and 40 mTorr, respectively. From these figures, it is clear that the temporal evolution of T_e is marginally dependent on the pressure in this range (20–40 mTorr). The electron temperature increases with applied RF pulse power during all three chosen phases. T_e increases from ~5 to ~9 eV during the stable 'on-phase' when the pulse power is varied from 100 to 500 W. During the stable 'off-phase', it increases from ~0.5 to ~3 eV. In CCP discharges, the sources

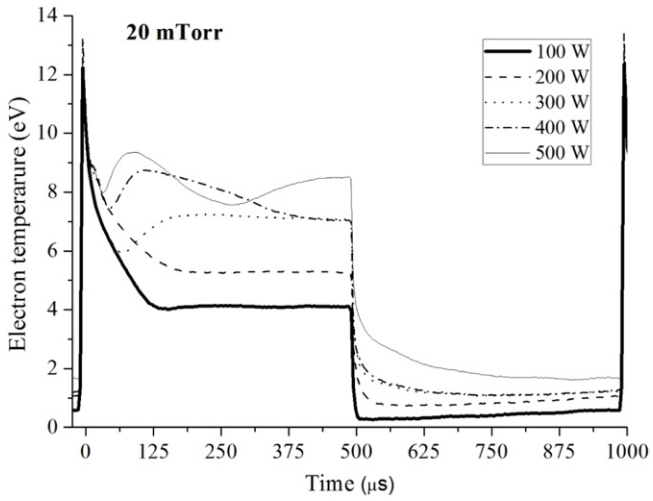

Figure 7. Electron temperature profile measured with the emissive probe for five different source powers at an average pressure of 20 mTorr. The discharge was pulsed at 1 kHz with 50% duty factor. The bias power was zero.

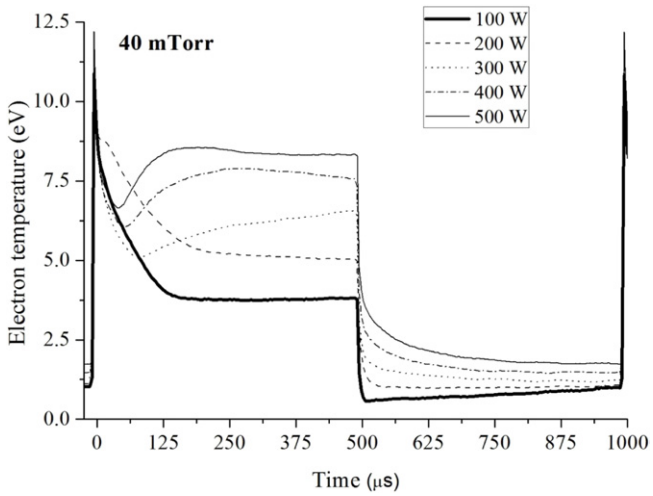

Figure 8. Electron temperature profile measured with the emissive probe for five different source powers at an average pressure of 40 mTorr. The discharge was pulsed at 1 kHz with 50% duty factor. The bias power was zero.

operating at high frequencies (such as 60 MHz) see the sheath capacitance as a short circuit. Therefore, a major part of the RF voltage applied at the electrode drops across the discharge body, where it produces ohmic dissipation, electron heating and ionization mechanism. It increases the plasma density and electron temperature, as observed in this study. The electron temperature increases with RF power, as reported earlier [6]. A slight decrease in electron temperature is also observed with increased pressure (20–40 mTorr) and it is consistent with the other reported data in DF-CCP discharges [6].

In addition to the general features observed in T_e evolution (figures 7 and 8), some structures in the on-phase, particularly at a high power (500 W), are observed. As the electron temperatures are calculated from the plasma potential profile, there is a finite possibility of inclusion of errors associated with the emissive probe technique. Therefore, the structure observed in the temporal dependence of electron temperature could be explained by the basic operating mechanism of the emissive probe.

The general feature in the temporal evolution of electron temperature (figures 7 and 8) is an initial overshoot and then a decrease in the electron temperature. After a few tens of μs (the exact time depends on the operating parameters, such as power and pressure), it decreases and attains a stable value. The fall time of the electron temperature decreases with RF power. This fall time is dependent on the electron plasma frequency and complex impedance of the measurement circuitry of the emissive probe. As the RF power increases, the plasma density (n_e) increases which, in turn, increases the electron plasma frequency (f_e). It results in a reduced electron characteristic time. This could be the reason for the observed decreasing T_e fall time with RF power.

A dip in the electron temperature is also observed, just after the initial overshoot, at high power (>300 W). As the power increases, the plasma density increases. To make the probe work at high plasma density, it should be in the strongly emitting condition and these emitting electrons may form a space charge region in front of the probe loop under certain conditions, such as the presence of a magnetic field and a low-density discharge. At the beginning of the discharge pulse, when the discharge evolves, the plasma density is low ($\sim 10^{12}$ m^{-3}). Therefore, the electrons emitted from the probe do not move into the plasma and make a space charge region in front of the probe loop. The probe loop, together with the space charge region, behaves like a virtual cathode and produces a dip in the plasma potential, and it also reflects on the electron temperature. Moreover, the emissive probe technique in floating mode provides only a qualitative analysis of the temporal evolution of T_e. For quantitative accuracy, there is a need to diagnose the discharge with other techniques such as a Langmuir probe.

A series of experiments were carried out to study the effect of RF biasing of the bottom electrode on the plasma potential evolution in the DF-CCP. Figures 9 and 10 show the temporal evolutions of the plasma potential within the pulse at two different pressures of 20 mTorr and 40 mTorr, respectively. Three RF powers of 100, 200 and 300 W in continuous wave (CW) mode were applied at the bottom electrode. A comparison of the figures (9 and 10) readily reveals that the plasma potential has a decreasing trend with pressure. At 300 W, the initial overshoot in the plasma potential reduces from 69 to 58 V when the pressure is increased from 20 to 40 mTorr. The plasma potential in the stable 'on-phase' also decreases from 43 to 35 V at the 300 W RF power level. This observed decreasing trend of plasma potential with pressure can be explained by Poisson's relation $V_p \propto (n_i - n_e)$, where n_i and n_e are the ion and electron densities, respectively. The charge particle mobility reduces with pressure and therefore the magnitude of $n_i - n_e$ decreases. This results in decreasing plasma potential with pressure. During the 'on-phase', the magnitude of V_p is marginally dependent on the applied biasing RF powers (100–300 W) and the trend of temporal evolution of V_p is similar at both pressures. However, the plasma potential evolution during the 'off- phase' has a significant dependence on the biasing power and pressure. It has an interesting feature

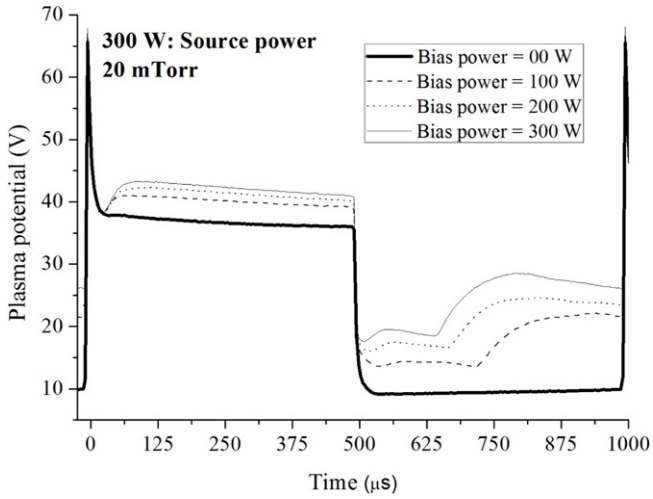

Figure 9. Plasma potential profile measured with the emissive probe for four different bias powers at an average pressure of 20 mTorr. The discharge was pulsed at 1 kHz with 50% duty factor. The source power was kept fixed at 300 W.

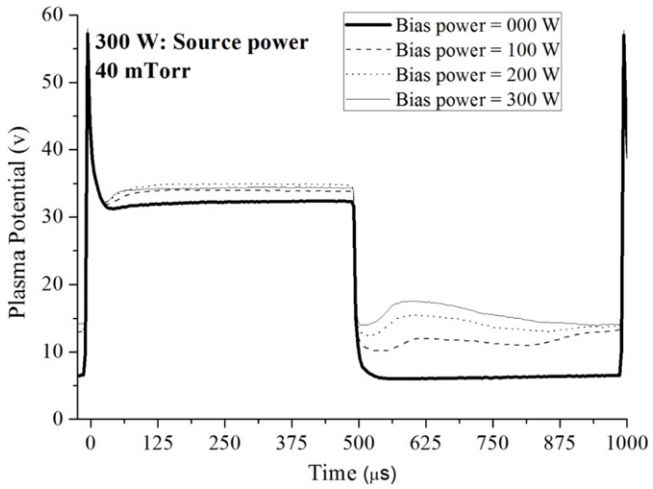

Figure 10. Plasma potential profile measured with the emissive probe for four different bias powers at an average pressure of 20 mTorr. The discharge was pulsed at 1 kHz with 50% duty factor. The source power was kept fixed at 300 W.

of development of a potential structure, which changes with the biasing power (see figure 9). V_p decreases rapidly after the pulse is switched off and attains a value of ∼13 V at the biasing power of 100 W. Then a small bump in V_p (∼1 V) appears at ∼30 μs after the pulse is switched off and then V_p remains stable for ∼210 μs after switching off the pulse. Then a second bump appears and V_p increases and achieves a value of ∼21 V at ∼390 μs after the switching off of the pulse and maintains it for the remaining pulse 'off-time'. The temporal emergence of the first and second bumps in the V_p profile, in the 'off-phase', linearly decreases with RF power (∼710–∼640 μs at 100–300 W bias power), as shown in figure 9. Comparing figures 9 and 10, it can be readily seen that the development of the second bump is also pressure sensitive and the magnitude (V) and time of its emergence reduce with pressure. The exact reason for the second bump observed in the 'off-phase' region in the V_p profile and its temporal emergence with power is not

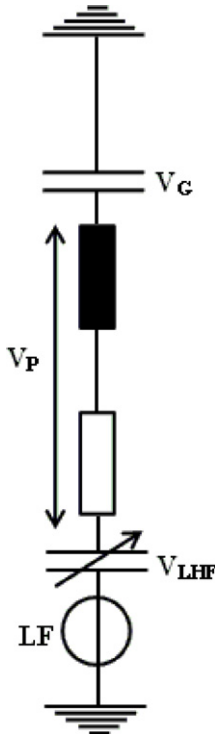

Figure 11. A schematic of the lumped element electrical equivalent circuit of the DF-CCP, when the top electrode is in the pulse 'off-time' and the bottom electrode is driven with RF power.

known and there is a need to carry out further investigations. However, it could be attributed to the changed discharge and sheath dynamics in the 'off-phase'.

The increase in plasma potential with the low-frequency power during the 'off-phase' can be explained on the basis of the lumped element electrical equivalent circuit of the DF-CCP shown in figure 11 [3, 40]. In this circuit, the electrode sheath is denoted by a non-linear capacitor, whereas the grounded sheath as a constant capacitor. The bulk plasma is represented as an L–R combination, where inductance and resistance represent electron inertia and ohmic dissipation, respectively. Figure 11 shows the top electrode grounded and the bottom electrode driven and it is equivalent to the pulsed top electrode in the 'off-phase' and bottom electrode driven, as in the region of discussion. As the RF pulse at the top electrode is switched off, the top electrode becomes grounded and the discharge could be treated as a single-frequency discharge. In CCP discharges, the lower frequency voltage drops mostly across the sheath; its peak value determines the dc sheath voltage and thus the plasma potential. Therefore, the higher the applied voltage (applied RF power) at the electrode, the higher will be the plasma potential, as observed in this study.

Figure 12 shows the temporal evolution of electron temperature with varying biasing power at the grounded electrode at 20 mTorr. From figure 12, it can be seen that the electron temperature increases (from 3 to 4 eV) in the pulse 'off-phase' of the top electrode. In DF-CCP discharges, the higher frequency power is used for electron heating and ionization, and the lower frequency is used to control the ion-bombarding energy onto the substrate. However, the effects produced by these frequencies are coupled [21, 29] and some

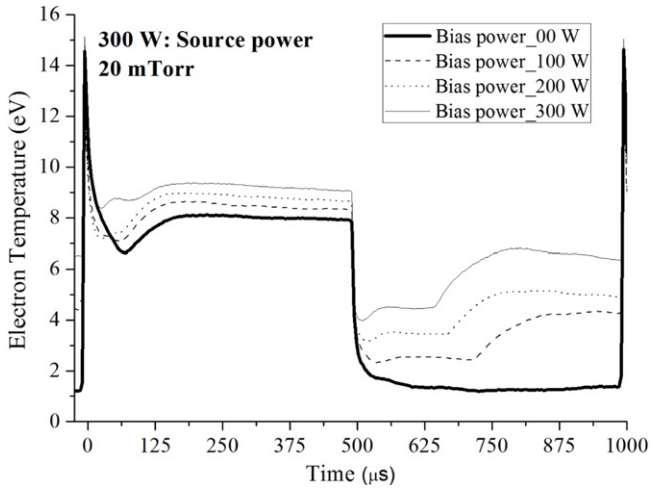

Figure 12. Electron temperature profile measured with the emissive probe for four different bias powers at an average pressure of 20 mTorr. The discharge was pulsed at 1 kHz with 50% duty factor. The source power was kept fixed at 300 W.

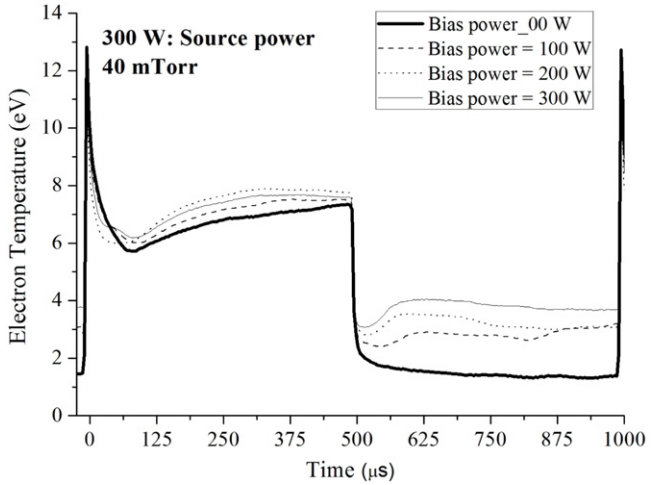

Figure 13. Electron temperature profile measured with the emissive probe for four different bias powers at an average pressure of 40 mTorr. The discharge was pulsed at 1 kHz with 50% duty factor. The source power was kept fixed at 300 W.

of the lower frequency is consumed in electron heating, which is responsible for the observed trend in electron temperature during the pulse 'off-phase' of the top electrode. From this observation, it can be concluded that, in a pulsed DF-CCP discharge, the effect of substrate biasing is more prominent in the 'off-phase' region of the top electrode when the substrate is biased by CW RF power.

Figure 13 shows the temporal evolution of electron temperature at 40 mTorr. The comparison of figure 12 and 13 readily reveals that the peak electron temperature decreases by ∼2 eV (from 15 to 13 eV) during the initial overshoot and by ∼1–2 eV in the 'on-phase' when the pressure is increased from 20 to 40 mTorr. The structure observed in electron temperature during the 'off-phase' at 20 mTorr diminishes with increasing pressure. This could be attributed to a change in discharge dynamics with pressure, and further investigation is needed to find out the exact reason.

4. Conclusions

Time-resolved plasma potential measurements were carried out in a pulsed dual-frequency CCP discharge (60 MHz/2 MHz) using an electron-emitting probe at two operating pressures of 20 and 40 mTorr. The pulsing frequencies were set at 1 kHz. The measurement region was the centre of the substrate, 10 mm above the substrate . It was observed that the main features observed in the V_p profile were similar, under all operating conditions—an initial overshoot, stable 'off-phase' and stable 'on-phase'. Under typical operational conditions (pressure 20 mTorr, pulse power of 500 W and pulsing frequency of 1 kHz), V_p overshoots to a positive value of 33 V and then attains a relatively stable value of 12 V (±2 V) in a time of 30 μs and sustains it during the remaining pulse 'on-time'. As the pulse is switched off, V_p decreases up to ∼3 V and remains stable during the whole pulse 'off-time'. The derived temporal evolution of electron temperature shows a high plasma potential (∼10 eV) in the 'on-phase' and a low T_e (∼3 eV) in the 'off-phase'.

It was also observed in this study that a CW RF biasing of the substrate significantly modulates the plasma potential evolution, specifically in the pulse 'off-time' region and the magnitude of modulation depends on the substrate biasing power. The magnitude of this modulation diminishes with the operating pressure.

Acknowledgments

This work was supported by the 'Development Program of Nano Process Equipments' of the Ministry of Knowledge Economy (L-2010-1438-000, Development of 450 mm plasma technology for low damage nano-device process).

References

[1] Kim H C and Lee J K 2004 *Phys. Rev. Lett.* **93** 085003
[2] Kawamura E, Lieberman M A and Lichtenberg A J 2006 *Phys. Plasmas* **13** 053506
[3] Mussenbrock T, Ziegler D and Brinkmann R P 2006 *Phys. Plasmas* **13** 083501
[4] Ohba T and Makabe T 2010 *Appl. Phys. Lett.* **96** 111501
[5] Huang X J, Xin Y, Yang L, Yuan Q H and Ning Z Y 2008 *Phys. Plasmas* **15** 113504
[6] Chen Z Y, Donnelly V M, Economou D J, Chen L, Funk M and Sundararajan R 2009 *J. Vac. Sci. Technol.* A **27** 1159
[7] Worsley M A, Bent S F, Fuller N C M and Dalton T 2006 *J. Appl. Phys.* **100** 083301
[8] Kim H C, Lee J K and Shon J W 2003 *Phys. Plasmas* **10** 4545
[9] Boyle P C, Ellingboe A R and Turner M M 2004 *Plasma Sources Sci. Technol.* **13** 493
[10] Boyle P C, Ellingboe A R and Turner M M 2004 *J. Phys. D: Appl. Phys.* **37** 697
[11] Dai Z L, Xu X and Wang Y N 2007 *Phys. Plasmas* **14** 013507
[12] Turner M M and Chabert P 2006 *Phys. Rev. Lett.* **96** 205001
[13] Turner M M and Chabert P 2006 *Appl. Phys. Lett.* **89** 231502
[14] Turner M M and Chabert P 2007 *Plasma Sources Sci. Technol.* **16** 364
[15] Chabert P, Levif P, Raimbault J L, Rax J M, Turner M M and Lieberman M A 2006 *Plasma Phys. Control. Fusion* **48** B231

[16] Wakayama G and Nanbu K 2006 *IEEE Trans. Plasma Sci.* **31** 638
[17] Tong L Z and Nanbu K 2006 *Europhys. Lett.* **75** 63
[18] Lee J K, Manuilenko O V, Babaeva N Yu, Kim H C and Shon J W 2005 *Plasma Sources Sci. Technol.* **14** 89
[19] Guan Z Q, Dai Z L and Wang Y N 2005 *Phys. Plasmas* **12** 123502
[20] Rauf S, Bera K and Collins K 2008 *Plasma Sources Sci. Technol.* **17** 035003
[21] Karkari S K and Ellingboe A R 2006 *Appl. Phys. Lett.* **88** 101501
[22] Li X S, Bi Z H, Chang D L, Li Z C, Wang S, Xu X, Xu Y, Lu W Q, Zhu A M and Wang Y N 2008 *Appl. Phys. Lett.* **93** 031504
[23] Hebner G A, Barnat E V, Miller P A, Paterson A M and Holland J P 2006 *Plasma Sources Sci. Technol.* **15** 879
[24] Semmler E, Awakowicz P and von Keudell A 2007 *Plasma Sources Sci. Technol.* **16** 839
[25] Ahn S K and Chang H Y 2009 *Appl. Phys. Lett.* **95** 111502
[26] Booth J P, Curley G, Maric D and Chabert P 2010 *Plasma Sources Sci. Technol.* **19** 015005
[27] Gans T, Schulze J, O'Connell D, Czarnetzki U, Faulkner R, Ellingboe A R and Turner M M 2006 *Appl. Phys. Lett.* **89** 261502
[28] Mishra A, Kelly P J and Bradley J W 2010 *Plasma Sources Sci. Technol.* **19** 045014
[29] Mishra A, Kelly P J and Bradley J W 2011 *J. Phys. D: Appl. Phys.* **44** 425201
[30] Chen F F and Chang J P *Principles of Plasma Processing* (Dordrecht/New York: Kluwer/Plenum)
[31] Yuan Q H, Xin Y, Yin G Q, Huang J, Sun K and Ning Z Y 2008 *J. Phys. D: Appl. Phys.* **41** 205209
[32] Godyak V A and Piejak R B 1990 *Phys. Rev. Lett.* **65** 996
[33] Kimura T and Noto M 2006 *J. Appl. Phys.* **100** 063303
[34] Kimura T and Ohe K 2002 *J. Appl. Phys.* **92** 1780
[35] Descoeudres A, Sansonnens L and Hollenstein Ch 2003 *Plasma Sources Sci. Technol.* **12** 152
[36] So S Y, Oda A, Sugawara H and Sakai Y 2002 *J. Phys. D: Appl. Phys.* **35** 2978
[37] So S Y, Oda A, Sugawara H and Sakai Y 2001 *J. Phys. D: Appl. Phys.* **34** 1919
[38] Sheehan J P, Raitses Y, Hershkowitz N, Kaganovich I and Fisch N J 2011 *Phys. Plasmas* **18** 073501
[39] Liu Y X, Zhang Q Z, Jiang W, Jing Hou L, Xiang-Zhan Jiang, Qi Lu W and You-Nian Wang 2011 *Phy. Rev. Lett.* **107** 055002
[40] Ziegler D, Mussenbrock T and Brinkmann R 2008 *Plasma Sources Sci. Technol.* **17** 045011
[41] Raitses Y, Staack D, Smirnov A and Fisch N J 2005 *Phys. Plasmas* **12** 073507
[42] Schrittwieser R, Ionita C, Balan P, Silva C, Figueiredo H, Varandas C A F, Rasmussen J J and Naulin V 2008 *Plasma Phys. Control. Fusion* **50** 055004